JOURNAL OF MATERIALS SCIENCE 24 (1989) 2871–2878

The abnormal grain growth and dielectric properties of (Nb, Ba) doped TiO_2 ceramics

C. J. CHEN, J. M. WU
Department of Materials Science and Engineering, National Tsing Hua University, Hsinchu, Taiwan

The effect of consolidation pressure and crystallite size of powders crystal phases of TiO_2 on sintered microstructure of TiO_2 ceramics doped with 0.25 mol% Nb and 1.0 mol% Ba were investigated. Also, the development sequence of abnormal grain growth of (niobium, barium) doped TiO_2 ceramics was proposed. The second phases of as-sintered surface were determined. The dielectric properties of Ag-electroded samples were correlated with the resistivity of the bulk (Nb, Ba) doped TiO_2 ceramics. Abnormal grain growth lowered the resistivity of bulk material of (Nb, Ba) doped TiO_2 ceramics, and moved the relaxation frequency of tan δ to high frequency region over 10^5 Hz. Controlling the sintered microstructures can obtain reasonably good dielectric properties.

1. Introduction

Yan and Rhodes [1] reported ultrahigh capacitance by doping Ta (or Nb) and Ba into TiO_2 ceramics. The space charge polarization occurring in the region of boundary segregation layer was thought to be the reason for the ultrahigh capacitance. Wu and Chen [2] studied the effects of barium and niobium on the dielectric properties of TiO_2 ceramics and found that the higher the amount of barium dopant, the more obvious the abnormal grain growth was, and the higher the relaxation frequency of tan δ was. But the relationship of sintered microstructure and dielectric properties of (Nb, Ba) doped TiO_2 ceramics was not discussed in depth, and was not clear yet. In the present paper the effect of consolidation pressure and starting crystal phases on controlling sintered microstructure will be studied and the influence of sintered microstructure on dielectric properties will be further analysed.

The initial stage of sintering of TiO_2 was studied by Anderson [3]. He concluded that the rate-controlling species in sintering of TiO_2 was oxygen vacancies. Edelson and Glaeser [4] discussed the role of particle substructure in the sintering of monosized titania, and proposed that the exaggerated intra-agglomerate crystallite growth resulted in the development of large grains in the early stage of sintering. However, the abnormal grain growth of TiO_2 in the later stage of sintering was not studied. The present paper will investigate the development of abnormal grain growth of (Nb, Ba) doped TiO_2 ceramics, and propose a model concerning the effects of consolidation pressure and starting crystal phases on abnormal grain growth.

2. Experimental procedures

The preparation of TiO_2 powders doping with barium and niobium started with reagent grade chemicals like $TiCl_4$ (Merck), $NbCl_5$ (Merck), and $BaCl_2 \cdot 2H_2O$ (Pipette). Liquid $TiCl_4$ was gradually dripped into deionized water. The temperature of the deionized water was about 4° C, and the volume of the deionized water used was five times that of the $TiCl_4$ liquid. After mixing $TiCl_4$ with deionized water, a white turbid solution was formed. By storing in a refrigerator kept at about 4° C for 24 h, the $TiCl_4$ aqueous solution became clear. Besides this, a $NbCl_5$ aqueous solution was made by dissolving $NbCl_5$ in a 35% HCl solution and then diluting it with deionized water; and a $BaCl_2$ solution was also prepared by adding $BaCl_2 \cdot 2H_2O$ into deionized water and stirring to complete dissolution. The prepared $TiCl_4$, $NbCl_5$, and $BaCl_2$ solutions were mixed together in desirable ratio equivalent to Ti : Ba : Nb = 100 : 1 : 0.25 in a beaker. Then, the mixed solution was slowly dripped into a 0.1 M aqueous solution of $(NH_4)_2CO_3$, which was adjusted with NH_4OH to pH = 9.5, to coprecipitate powders containing Ti, Ba and Nb. The pH value of the co-precipitating solution was kept at 9.5 by adding suitable NH_4OH solution slowly into the reaction beaker during the co-precipitation process. After the reaction was completed, the co-precipitated powders was filtered and washed with deionized water three times, followed by washing with 99.5% ethyl alcohol and filtered twice. The washed powder was dried with an infrared lamp, and then calcined at 950 and 600° C for 1.5 h, respectively. The phase of powder which calcined at 950° C was rutile, and that calcined at 600° C was anatase. After calcination, three powders were prepared: 100A (100% anatase), 50R (50% rutile and 50% anatase), and 100R(100% rutile). The powders were ball-milled with ZrO_2 balls in deionized water in a plastic jar for 3 h with addition of 1.0 wt% PVA (polyvinyl alcohol). After ball-milling, the powders were dried, pulverized, and forced to pass no. 120 sieve for granulation. The granulated powder was weighted as 0.3 g per sample and then dry pressed at

0022–2461/89 $03.00 + .12

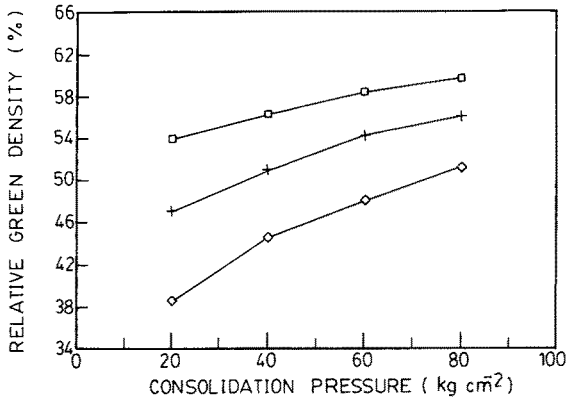

Figure 1 Dependence of relative green density on consolidation pressure for (◇) 100A, (+) 50R and (□) 100R.

four different pressures which appeared on the presser indicator as 80, 60, 40 and 20 kg cm^{-2} respectively, and the samples will be represented with symbol: 80 kg, 60 kg, 40 kg and 20 kg respectively. The true calculated consolidation pressures on the die of 1 cm diameter corresponded to 158, 119, 79 and 40 MPa, respectively. The pellets were sintered at 1350° C for 2 h in air with a heating rate of 10° C min^{-1}, and then cooled at a rate of 4.7° C min^{-1} [5].

For dielectric property measurements, two types of electrodes were prepared on the sample discs. Silver electrodes were made on both surfaces of the sintered pellets by coating silver paste on pellet surfaces, baking at 300° C for 5 min, soaking at 550° C for 15 min, and cooling in the furnace. Aluminium electrodes were vacuum evaporated on both disc surfaces. The relative dielectric constant and dielectric dissipation factor were measured with an LCR (Inductance, Capacitance, Resistance) meter (Cheng-Hua) in the frequency range from 10 to 10^5 Hz.

For studying the abnormal grain growth of (Nb, Ba) doped TiO_2 ceramics, we sintered the pellets of 100A80kg, which was made from 100A powder and the consolidation pressure on the presser indicator was 80 kg cm^{-2}, at four temperatures, 1050, 1150, 1250 and 1350° C for 2 h, and at 1350° C for different sintering time, 0, 1, 2 and 8 h.

The impurities were analysed with ICP-AES. The results, which were listed in a previous paper [2] and will not be shown here, showed that the concentrations of representative impurities were reasonably low and should not cause problems.

3. Results and discussion

3.1. General

Figure 1 illustrates the relative green density dependence of consolidation pressure for various ratios of rutile to anatase starting powders. Higher consolidation pressure results in higher relative green density. The green density also increases with the content of rutile phase. Figures 2a and b show the SEM (scanning electron microscope) images of the morphology of the rutile and anatase particles. The large agglomerates of rutile phase, about 10–30 μm, are two or three times of the size of anatase phase, about 5–10 μm. Thus, the higher ratio of rutile starting phase resulted in a higher relative green density.

The variations of the green density and of the ratio of rutile to anatase in the starting powder are expected to develop different sintered microstructures. Furthermore, the microstructures affect the dielectric properties of samples. The second phases of as-sintered surface vary with starting phase of TiO_2. This section will discuss these effects individually.

3.2. Abnormal grain growth and the effect of consolidation pressure

Abnormal grain growth was found in (Nb, Ba) doped TiO_2 ceramics [2, 5, 6], but was not discussed in depth. In the present investigation, 100A80kg green bodies were sintered at different temperature and different sintering time which produced different sintered microstructures for studying the development of abnormal grain growth of (Nb, Ba) doped TiO_2 ceramics. Figures 3a to d illustrate the microstructures of the as-sintered surfaces of the 100A80kg samples sintered at different temperatures, 1050, 1150, 1250 and 1350° C, with the same sintering time of 2 h. The grain size of the sample sintered at 1050° C is relatively uniform, about 0.2 μm, and interagglomerate densification and neck growth develop reasonably well. There are a few pores left between agglomerates. However, the microstructure of the sample sintered at 1150° C is the pore free, and the grain size distribution

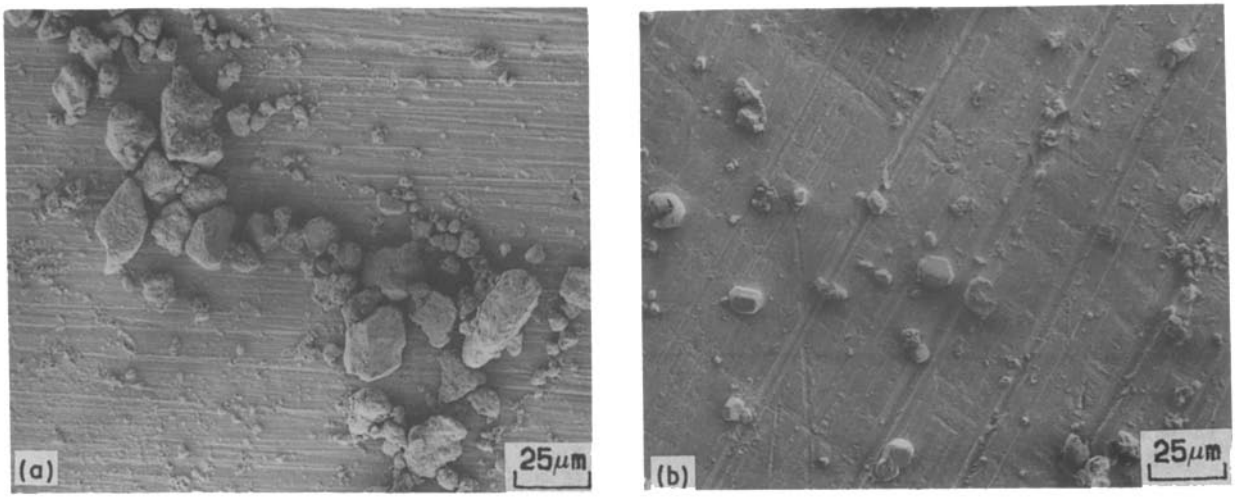

Figure 2 SEM images of the morphology of particles with different starting phase, (a) rutile (b) anatase.

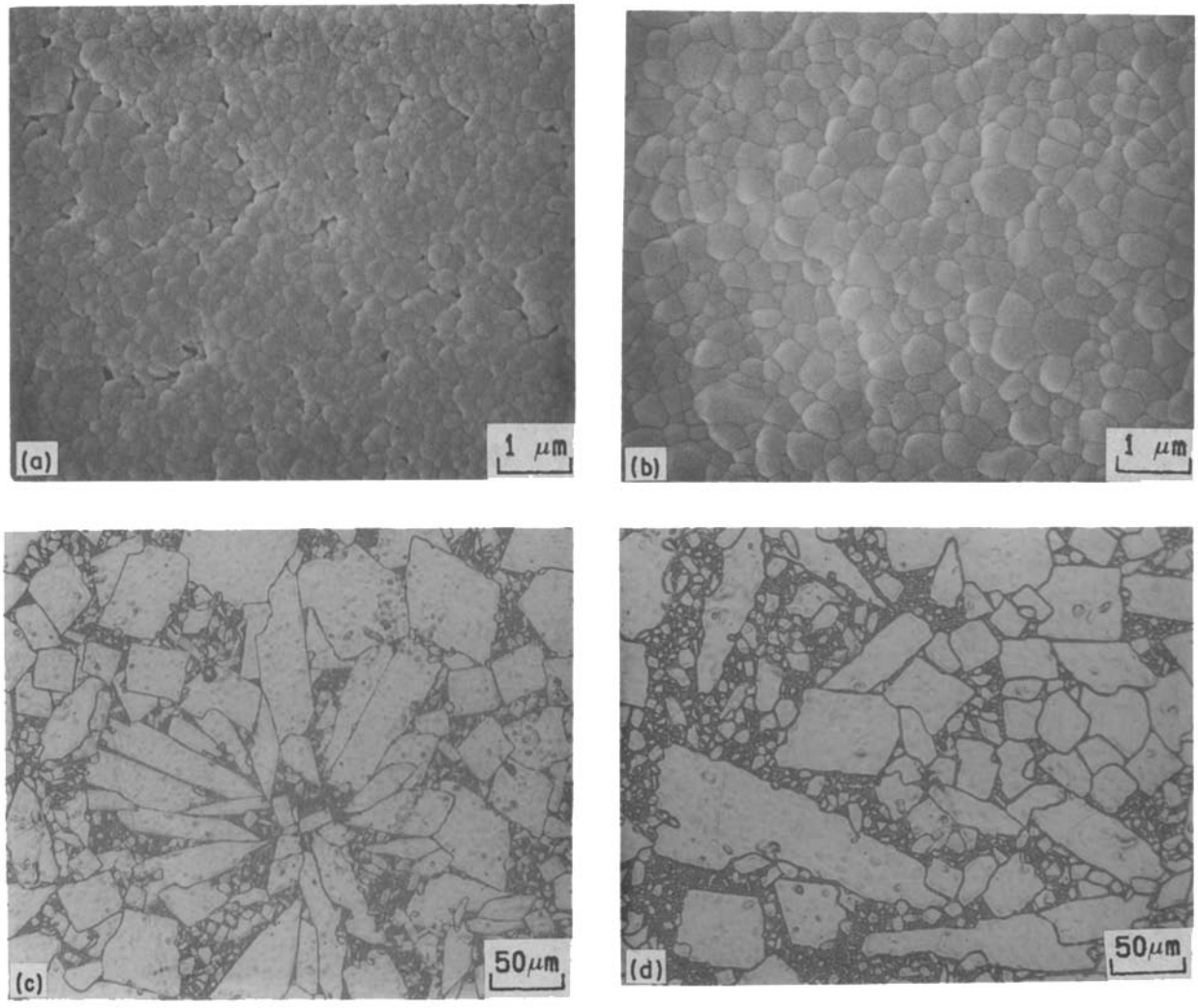

Figure 3 As-sintered surface of 100A80kg samples sintered at (a) 1050° C, (b) 1150° C, (c) 1250° C and (d) 1350° C for 2 h. (a) and (b) are SEMs; (c) and (d) are optical micrographs.

becomes broad. The size of large grains are about 0.7 μm, however, that of small grains are about 0.2 μm. Abnormal grain growth happened when samples were sintered above 1250° C for 2 h. As the sample heated to 1350° C and cooled down immediately, whose microstructure is not shown, the abnormal grain growth is a little more prominent than that of the sample sintered at 1250° C for 2 h. When the sintering time was prolonged for 1, 2 and 8 h at 1350° C, the abnormal grains grew larger.

Below 1050° C intra-agglomerate densification and grain growth compete with interagglomerate densification and neck growth. As the temperature was raised up to 1150° C the interagglomerate densification was more complete and the grain growth within agglomerate kept on going, therefore, the grain size distribution became broad. The larger grains are the sources of abnormal grain growth. The abnormal grain growth occurred rapidly at 1250° C. The size of abnormal grains are about 50–100 μm which are larger than the size of the large agglomerates of starting powder by one order of magnitude, and the normal grain size are about several micrometres. To achieve this, the larger grain within agglomerates must grow crossing into other agglomerates and consume the grains of the other agglomerates to develop the microstructures of abnormal grain growth. As the abnormal grain growth have been developed, raising the sintering temperature or prolonging the sintering time results in higher degree of abnormal grain growth.

The microstructures of the 100A and 50R samples were very sensitive to the powder packing condition. From the sintered microstructures which were shown in Figs 4 and 5, higher consolidation pressure gave more prominent abnormal grain growth. The low consolidation pressure sample, 20 kg cm^{-2}, gave only slight abnormal grain growth. The large grains whose size were about 2–10 μm were almost of the same size as the agglomerates of the starting powder. When consolidation pressure was higher than 20 kg cm^{-2}, i.e. higher green density and closer agglomerate arrangement observed from SEM images, the sintered microstructures have high extents of abnormal grain growth. The sizes of the large abnormal grains were about 50–150 μm which were larger than the agglomerates of the starting powder by one order of magnitude.

The looser packing of the agglomerates slowed down the rate of interagglomerate densification and neck growth, which would be slower than that of intra-agglomerate densification and grain growth. However, some crystallites within agglomerates still grow into large grains. When the larger grain within

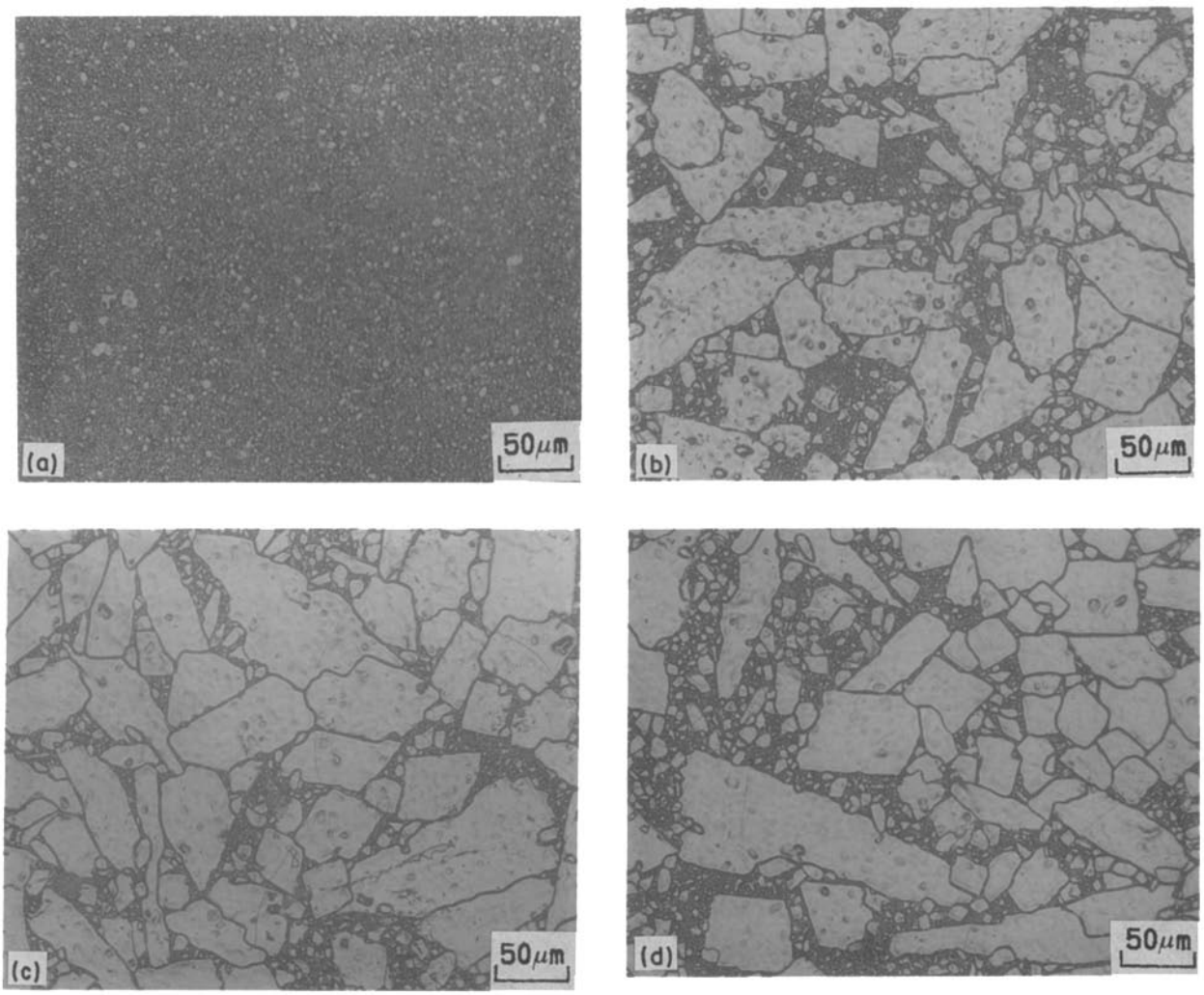

Figure 4 As-sintered surface of the 100A samples with different consolidation pressure (a) 20 kg, (b) 40 kg, (c) 60 kg and (d) 80 kg.

agglomerate developed, the grain size would exceed the interagglomerate neck size. Consequently, the grain growth crossing into another agglomerate became very difficult because of increasing grain boundary area. Edelson and Glaeser [4] proposed that under this condition the interagglomerate grain growth was inhibited. Therefore, one agglomerate would develop into one or several grains. This was the condition for the microstructures of samples of 100A and 50R with low consolidation pressure. As the sintering time proceeded or temperature was raised, the inter-agglomerate densification and neck growth were almost completed. And second phases precipitated between grain boundaries, inhibiting grain growth. If the grain size was roughly uniform and there existed second phases between grain boundaries, then the abnormal grain growth would not have happened. Thus, the final grain size was similar to the particle size distribution of the initial powder. The closer agglomerates promote the inter-agglomerate densification and neck growth, and therefore promote the abnormal grain growth. Identically, the small crystallite size of the starting powder accelerated the inter-agglomerate densification and neck growth, and this will be discussed in the next section. Since the two effects promote the abnormal growth, the rate of inter-agglomerate densification and neck growth are thought to be very important for abnormal grain growth.

In summary we propose three stages of abnormal grain growth for (Nb, Ba) doped TiO_2 ceramics. (1) Intra-agglomerate densification and grain growth develop large grains. If the interagglomerate densification and neck growth is fast enough as compared with intra-agglomerate densification and grain growth, then (2) large grains within agglomerates grow crossing into the other agglomerates, developing abnormal grains, and (3) abnormal grains continue to grow larger.

The grain sizes and sintered microstructures of the 100R samples with various consolidation pressures were almost the same and are shown in Figs 6a to d. These results seem to violate the previous argument, however, they can be explained by the existence of second phases in the 100R starting powder, which were confirmed by X-ray powder diffraction. The second phases inhibited grain growth. If the driving force of grain growth was not strong enough to overcome the drag force due to the second phases existing between grain boundaries, then only slight grain growth within the agglomerate could be expected. The grain size of the samples of 100R for various consolidation pressures was about 1–5 μm which was smaller than the size of the large agglomerates of the starting powder. Therefore, grain growth was restricted within agglomerates with little chance to grow crossing the agglomerates to develop abnormal grain growth.

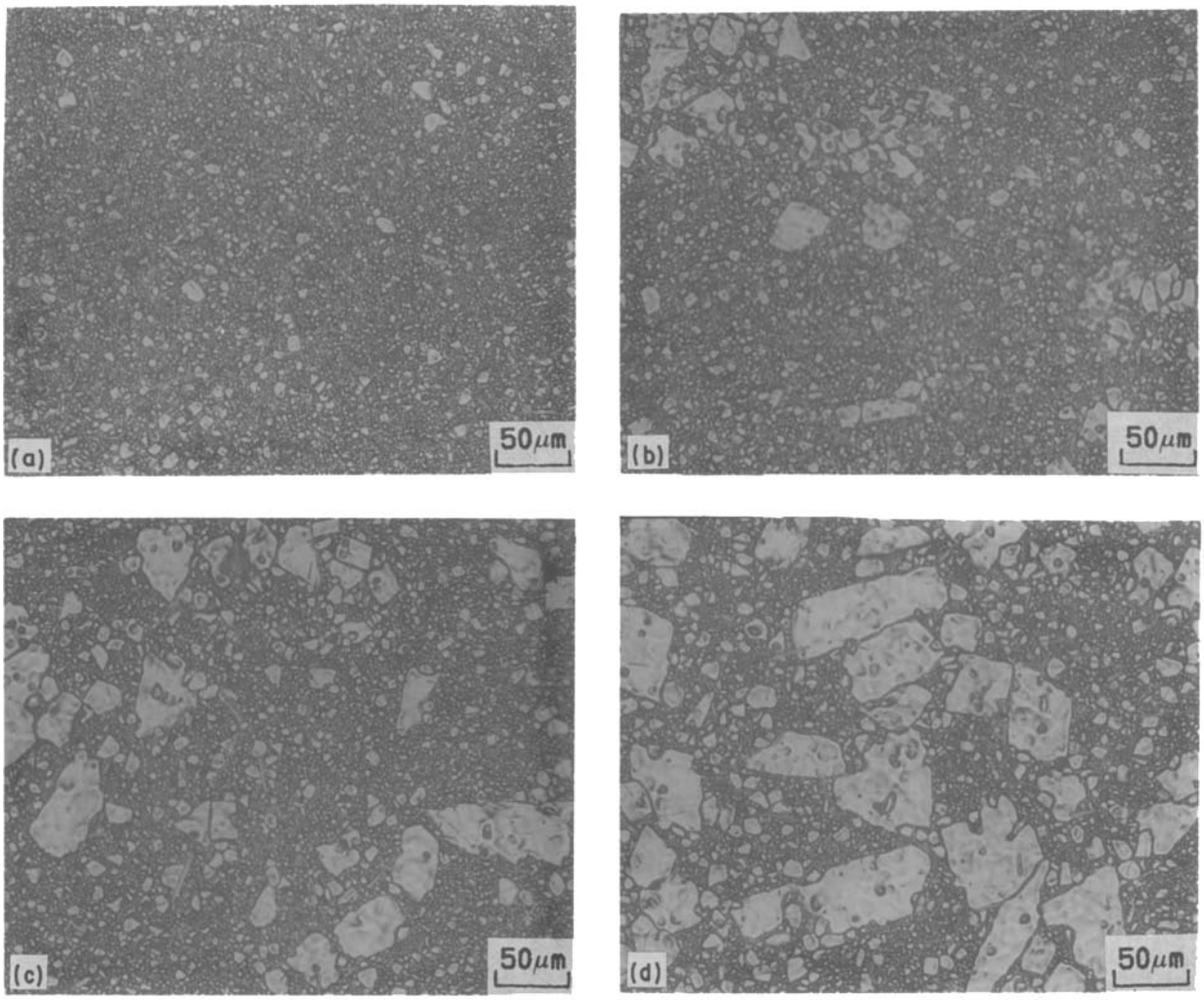

Figure 5 As-sintered surface of the 50R samples with different consolidation pressure (a) 20 kg, (b) 40 kg, (c) 60 kg and (d) 80 kg.

3.3. Influence of powder characteristic on sintered microstructure

When sintering behaviour is considered, the crystallite size of the starting powder cannot be ignored. The crystal phase was anatase as the co-precipitation powder was calcined at 600° C, while the crystal phase was rutile as calcined at 950° C. High calcination temperatures promote crystallite growth. From the observation of SEM the crystallite size of rutile phase was about 0.2 μm. However, the crystallite size of anatase phase, which was about 40 nm from the SEM image and XRD line broadening, was rather smaller than that of rutile phase.

Figure 7 shows the dependence of the average grain size and the d.c. resistivity ϱ_0 (assumed $\varrho_0 \simeq \varrho(12\,\text{Hz})$ explained in Section 3.5) of the bulk sample on consolidation pressure for different mixing ratio of rutile to anatase. The average grain size was virtually proportional to consolidation pressure, and the d.c. resistivity was just the opposite. The average grain size indicates the degree of abnormal grain growth. The anatase phase starting powder promoted abnormal grain growth as the consolidation pressure was larger than 20 kg cm^{-2}. This is because the crystallite size of the anatase powder was rather smaller than that of rutile powder, so that the driving force of grain growth within agglomerates of anatase starting powder was larger than that of rutile powder in the early stage of sintering. And the inter-agglomerate densification and neck growth were more rapid for anatase starting powder. The large grain within agglomerates are more likely to proceed abnormal grain growth. In contrast, the driving force of grain growth for rutile starting powder was smaller than that of anatase. Therefore, the degree of abnormal grain growth was proportional to the content of the anatase starting phase.

3.4. Variation of the formation of secondary phases with starting phase of TiO_2

Secondary phases, had been found $BaTi_4O_9$ and $Ba_2Ti_9O_{20}$, on the as-sintered surface and interior of TiO_2 doped with BaO [7]. O'Bryan and Yan [7] found that the blocklike, equiaxed prisms were $Ba_2Ti_9O_{20}$, and acicular prisms and large transparent grains were $BaTi_4O_9$. In that paper [7] the ceramic samples were prepared from high-purity TiO_2 (anatase) and $BaTiO_3$. Nevertheless, in this work the compound of second phases seem dependent on the crystal phase of the starting powder. Table I listed the secondary phases, which were identified by XRD, of the as-sintered surface for various conditions. Rutile starting phase favoured the formation of $Ba_2Ti_9O_{20}$, and anatase favoured $BaTi_4O_9$. $BaTi_4O_9$ and $Ba_2Ti_9O_{20}$ coexist in the sample sintered from mixed powder of rutile and anatase starting phase. The shape of $BaTi_4O_9$ was of

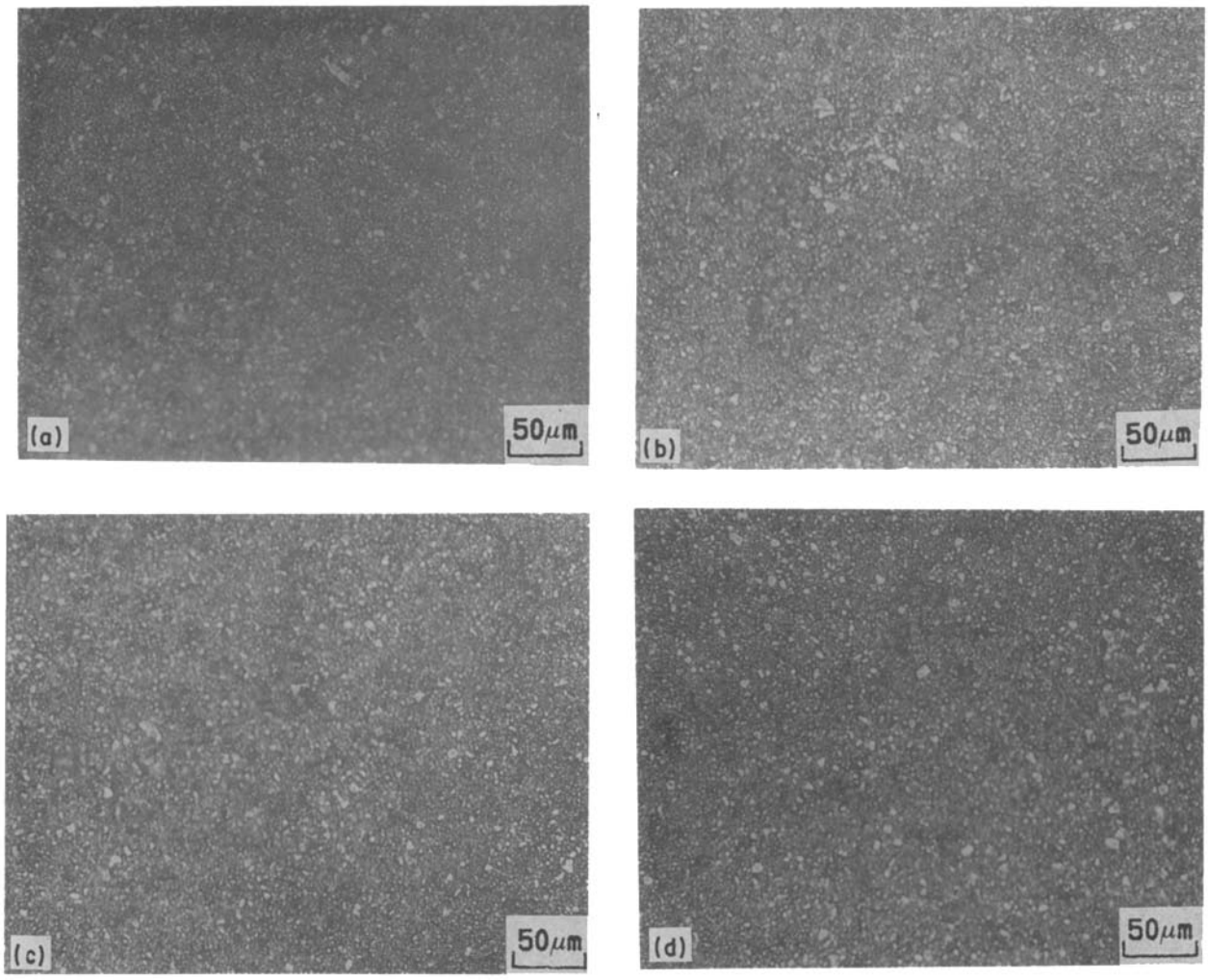

Figure 6 As-sintered surface of the 100R samples with different consolidation pressure (a) 20 kg, (b) 40 kg, (c) 60 kg and (d) 80 kg.

long-rods of length about 50–150 μm, and that of $Ba_2Ti_9O_{20}$ was blocklike.

Prolonging sintering time at 1350° C increased the amount of secondary phases of the as-sintered surface because barium diffuses from the interior of the sample to surface during sintering. The ionic radius of Ba^{+2} was much larger than that of Ti^{+4}. As Ba^{+2} substituted Ti^{+4} there existed very large elastic energy around the sublattice [8]. For the sake of elastic energy relaxation barium diffused from grain bulk to grain boundaries or sample surfaces forming secondary phases. The diffusion process was very rapid because of the high diffusivity of barium in TiO_2 [7].

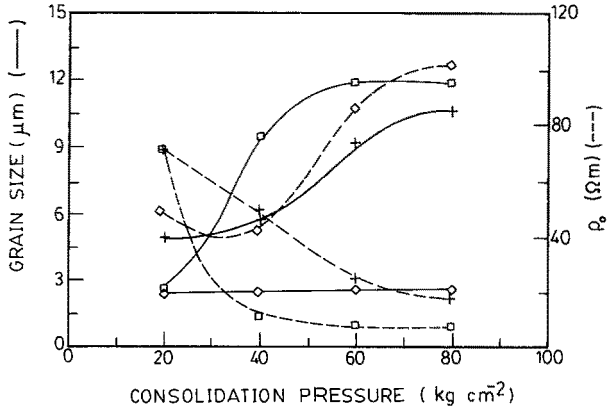

Figure 7 Dependence of the average grain size and ϱ_0 on consolidation pressure for different mixing ratio of rutile to anatase. (□) 100A, (+) 50R, (◇)100R.

3.5. Dependence of dielectric properties on microstructure

The sintered density of samples with various starting phase and different consolidation pressure are all above 96% of the theoretical density. Figs 8a to c show the variation of tan δ with frequency for samples coated with Ag-electrode for different consolidation pressures and various mixing ratios of rutile to anatase phase. There are no peaks of tan δ observed in the range of measuring frequency ($10–10^5$ Hz) for those samples with average grain size larger than 9 μm, which have obvious abnormal grain growth. Therefore,

TABLE I Secondary phases of the as-sintered surface for various conditions

	100R	50R	100A
20 kg	$Ba_2Ti_9O_{20}$	$BaTi_4O_9$ + *$Ba_2Ti_9O_{20}$	$BaTi_4O_9$
40 kg	$Ba_2Ti_9O_{20}$	$BaTi_4O_9$ + *$Ba_2Ti_9O_{20}$	$BaTi_4O_9$
60 kg	$Ba_2Ti_9O_{20}$	$BaTi_4O_9$ + *$Ba_2Ti_9O_{20}$	$BaTi_4O_9$
80 kg	$Ba_2Ti_9O_{20}$	$BaTi_4O_9$ + *$Ba_2Ti_9O_{20}$	$BaTi_4O_9$

*Small amount.

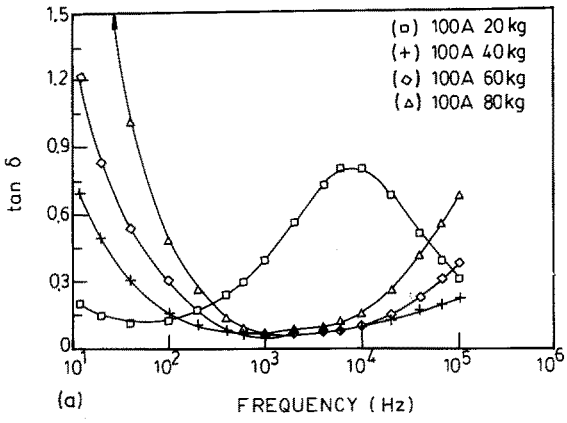

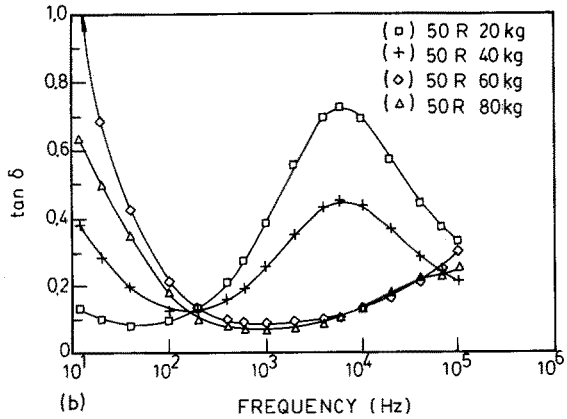

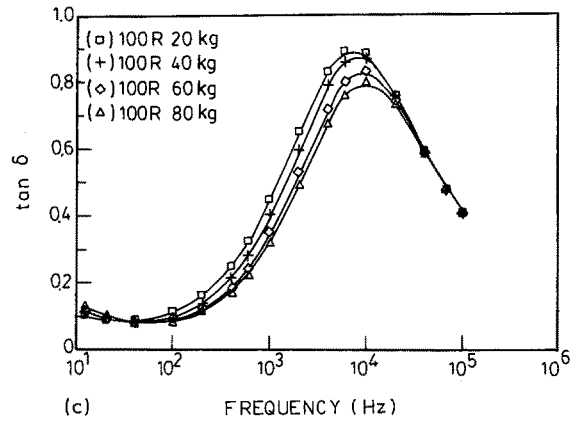

Figure 8 Frequency dependence of tan δ for the samples of different mixing ratio of rutile to anatase (a) 100A, (b) 50R and (c) 100R. These samples were coated with silver electrodes.

the high content of anatase starting phase as well as the high consolidation pressure cause higher relaxation frequency of tan δ. The dielectric properties presented in the present paper were measured with Ag-electrode, while d.c. resistivities were measured with Al-electrode.

Wu and Chen [2] proposed an equivalent circuit for specimens as a series of three RC (Resistance and Capacitance) sections which represent grains, grain boundary layers, and electrodes. The grain boundary were not effective barriers for electron carriers [2]. The sections representing the grain and the grain boundary layers can be further combined as material section. The circuit can be simplified as a series of the RC section of material and that of electrode. Silver paste was not in ohmic contact on n-type TiO_2 [2], thus the electrode section can not be ignored. The interface between the silver electrode and the ceramic blocked electron carriers which migrated within the TiO_2 ceramics, resulting in space charge accumulation. The dielectric properties of the samples with a silver electrode resulted from combinations of the ceramics and the electrode–ceramics interface. In contrast, an evaporated aluminium electrode was in ohmic contact on n-type TiO_2 [9]. The electrode section can be ignored, the dielectric properties reflected the material properties of TiO_2 ceramics. Since the lowest frequency available in the present investigation, 12 Hz, is close to the d.c. field, and the relative dielectric constant and resistivity vary only slightly in the low frequency region, we assume $K_0 \simeq K$ (12 Hz) for Ag-electroded samples and $\varrho_0 \doteq \varrho$ (12 Hz) for Al-electroded samples, where K = relative dielectric constant, Df_0 = dissipation factor at 0 Hz. For convenience we assume Df_0 represents virtually the conduction loss of the whole specimen. By plotting K_0 and Df_0 against ϱ_0 in Figs 9 and 10, they show that K_0 and Df_0 are inversely proportional to ϱ_0 except Df_0 vs ϱ_0 for 100R, which is almost constant of about 0.1 for various ϱ_0. The grain boundaries of (Nb, Ba) doped TiO_2 ceramics were back to back Schottky barriers [2, 6]. According to Schottky barrier model ln ϱ_0 was inversely proportional to the average grain size of the ceramics. As the degree of abnormal grain growth increased, the average grain size increased, therefore the resistivity of the ceramics decreased exponentially. The resistivity of the ceramics is inversely proportional to the

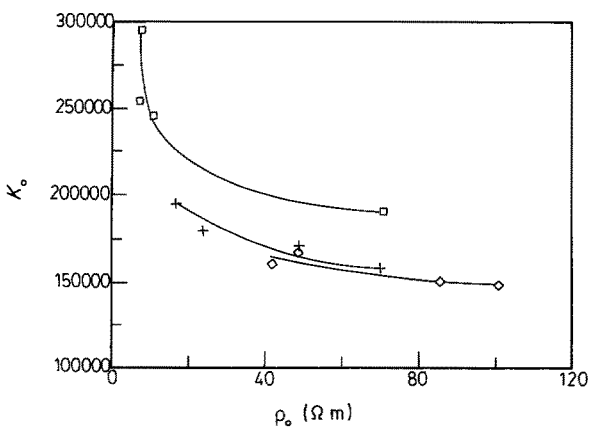

Figure 9 K_0 as a function of ϱ_0 for different mixing ratio of rutile to anatase. (□) 100A, (+) 50R, (◇) 100R.

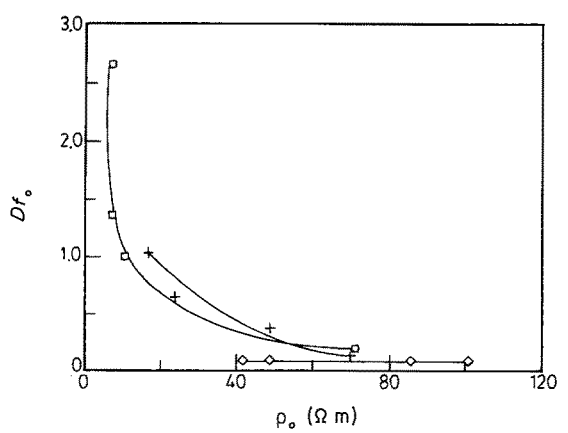

Figure 10 Df_0 as a function of ϱ_0 for different mixing ratio of rutile to anatase. (□) 100A, (+) 50R, (◇) 100R.

concentration of the electron carriers which can move across the sample. As silver paste is employed as the electrodes, which are non-ohmic contacts on n-type TiO_2 ceramics, the electron carriers are blocked at the electrode–ceramics interface. Thus, the ceramics with low resistivity accumulated a higher concentration of electron carriers beneath the electrode–ceramic interface, and elevated the probability of electron carriers going beyond the electrode–ceramic interface, therefore, conduction loss was raised. The ceramics with obvious abnormal grain growth have no peaks of tan δ in the range of measuring frequency, and have high relative dielectric constant and high conduction loss. Moreover, the relative dielectric constant dependence of frequency was more stable in the range of measuring frequency for the ceramics with higher relaxation frequency, and the relative dielectric constant was about 1.5–2 $\times$ 10^5 and tan δ was about 0.06 at 1 kHz.

The dielectric properties are strongly affected by the resistivity of the ceramics and by the interface between the electrode and the ceramics. The relaxation frequency of tan δ affects the dispersion of the ultrahigh capacitance. It is beneficial to discuss the relationship between the relaxation frequency of tan δ, the resistivity of the ceramics, and the relative dielectric constant of electrode–ceramic interface. The relaxation frequency f_r [2] can be given as:

$$f_r = \frac{2(1 + K)^{1/2}\varepsilon_0}{(2k_1 + k_2)\varrho_2} = \frac{\text{constant}}{\varrho_2} \quad (1)$$

where

$$K = \frac{9vk_1}{2k_1 + k_2}$$

k_1, k_2 are the relative dielectric constants of the grain boundary layer and grain, respectively, ϱ_2 the resistivity of grain, v the volume fraction of grain, ε_0 the dielectric permittivity of vacuum.

The Ag-electroded sample can be simplified as series of RC section of the ceramics and that of electrode–ceramic interface. Because the effect of the interface cannot be ignored, and the resistivities of the ceramic are low enough to be thought of as semiconductor. The subscripts 1 and 2 in Equation 1 stand for the electrode interface and the ceramic, respectively. Therefore, the relaxation frequency of tan δ was also inversely proportional to the resistivity of the ceramic. The relaxation frequency of tan δ was inversely proportional to the resistivity of the ceramic from experimental data except the samples of 100R. This result is rather consistent with the Equation 1. The resistivities of 100R increase with the samples consolidation pressure, nevertheless, relaxation frequency are almost the same, about 10 kHz.

4. Conclusion

1. High consolidation pressure resulted in high relative green density and raised the probability of abnormal grain growth.

2. Higher content of anatase starting powder resulted in a higher degree of abnormal grain growth. The sintered microstructures of 100R which have only slight abnormal grain growth are almost independent of the consolidation pressure.

3. The secondary phases of the as-sintered surface of rutile starting phase favour $Ba_2Ti_9O_{20}$, but those of anatase phase favour $BaTi_4O_9$.

4. The K_0 and conduction loss are raised by abnormal grain growth. The ceramics with obvious abnormal grain growth, whose average grain size are larger than 9 μm, have high relaxation frequency of tan δ. The relaxation frequency of tan δ was inversely proportional to the resistivity of the ceramics except the samples of 100R.

5. The crystallite size of anatase phase starting powder was about 40 nm, and that of rutile phase starting powder was about 0.2 μm. The driving force of grain growth of anatase phase starting powder was stronger than that of rutile phase starting powder. If the rate of inter-agglomerate densification and neck growth is fast enough as compared with that of intra-agglomerate densification and grain growth, then the abnormal grain growth will be promoted. With controlled sintered microstructure, the (Nb, Ba) doped TiO_2 ceramics with Ag-electrode would have an ultrahigh relative dielectric constant and reasonably low tan δ.

Acknowledgements

The authors acknowledge the support of the National Science Council of the Republic of China under the contract NSC 77-0404-E007-01.

References

1. M. F. YAN and W. W. RHODES, Advances in Ceramics Vol. 7, "Additives and Interfaces in Electronic Ceramics", edited by M. F. Yan and A. H. Heuer (The American Ceramic Society, Columbus, Ohio, 1983) p. 226.
2. J. M. WU and C. J. CHEN, *J. Mater. Sci.* **23** (1988) 4157.
3. H. U. ANDERSON, *J. Amer. Ceram. Soc.* **50** (1967) 235.
4. L. H. EDELSON and A. M. GLAESER, *ibid.* **71** (1988) 225.
5. J. M. WU and H. M. SUNG, *Mater. Sci. Eng.* in press.
6. J. M. WU and C. J. CHEN, *J. Mater Sci.* in press.
7. H. M. O'BRYAN and M. F. YAN, *J. Amer. Ceram. Soc.* **65** (1982) 615.
8. M. F. YAN, R. M. CANNON and H. K. BOWEN, Advances in Ceramics Vol. 6, "Character of Grain Boundaries", edited by M. F. Yan and A. H. Heuer (The American Ceramic Society, Columbus, Ohio, 1983) p. 255.
9. O. W. JOHNSON and J. W. DEFORD, *J. Appl. Phys.* **43** (1972) 807.

Received 18 July
and accepted 21 November 1988